EURASIP Journal on Applied Signal Processing 2002:7, 679–685

Spatial and Spectral Methods for Weed Detection and Localization

Jean-Baptiste Vioix
UMR CPAP ENESAD CEMAGREF 21, boulevard Olivier de Serres, 21800 Quetigny, France
Email: jb.vioix@enesad.fr

Jean-Paul Douzals
UMR CPAP ENESAD CEMAGREF 21, boulevard Olivier de Serres, 21800 Quetigny, France
Email: jp.douzals@enesad.fr

Frédéric Truchetet
Le2i, IUT Le Creusot 12, rue de la Fonderie, 71200 Le Creusot, France
Email: f.truchetet@iutlecreusot.u-bourgogne.fr

Louis Assémat
INRA, Unité de Malherbologie et Agronomie, BP 86510 21065 Dijon Cedex, France
Email: assemat@dijon.inra.fr

Jean-Philippe Guillemin
ENESAD laboratoire CBF, 21 boulevard Olivier de Serres, 21800 Quetigny, France
Email: jp.guillemin@enesad.fr

Received 26 July 2001 and in revised form 7 February 2002

This study concerns the detection and localization of weed patches in order to improve the knowledge on weed-crop competition. A remote control aircraft provided with a camera allowed to obtain low cost and repetitive information. Different processings were involved to detect weed patches using spatial then spectral methods. First, a shift of colorimetric base allowed to separate the soil and plant pixels. Then, a specific algorithm including Gabor filter was applied to detect crop rows on the vegetation image. Weed patches were then deduced from the comparison of vegetation and crop images. Finally, the development of a multispectral acquisition device is introduced. First results for the discrimination of weeds and crops using the spectral properties are shown from laboratory tests. Application of neural networks were mostly studied.

Keywords and phrases: weed detection, spatial analysis, spectral analysis, Gabor filter, neural network, image processing.

1. INTRODUCTION

Weed detection is extensively studied, as herbicide application has a relevant impact on farm economics and environment. Developing a spraying strategy in the context of precision agriculture needs to improve in-field detection of weeds. According to literature, weed detection using image analysis was directed through different approaches. First experimental works were based on the spectral signature of weeds and crops. Vrindts and de Baerdemaeker [1] determined some specific spectral bands to achieve weed identification. Statistical analyses were conducted to find spectral properties of each species. In the same way Pollet et al. [2] developed an imaging spectrograph. This device gave an image with the spatial dimension on vertical axis and the spectral dimension on horizontal axis. Another experimental method was based on morphological properties extracted from leaf shape using simple geometric shape factors (elongation, diameter, etc.) [3, 4]. In the same way Manh et al. used deformable templates to modelize leaf shape [5, 6]. In these two last cases, high resolution images were needed. Moreover, computation time was very important and limited that last application to small area investigation. In-field detection of weeds was also possible on stubble. For example, Biller et al. [7] achieved a sensor to detect plants on bare soil. In this case, two optical bands as red (650 nm) and infrared (850 nm) were used to find vegetation . The difference between the two reflectances allowed online spray-

ing control. Finally, last approach concerned remote sensing imaging. For example, aerial images taken with four cameras equipped with optical band-pass filters were used by Rew et al. [8] to discriminate weeds and crops. Weeds were detected by a significant increase in NDVI (normalized difference vegetation index). All these previous approaches were conducted in order to discriminate weeds and crops from their spectral signature or shape. The objective of this paper is to develop spatial then spectral methods upon aerial photographies in order to improve weed detection and localization.

2. ACQUISITION AND PREPROCESSING

2.1. Image acquisition for spatial investigation

A remote control aircraft was customized for this application. An Olympus μII film[1] camera was placed in the hold; the shot was manually triggered through the remote control. A miniature video camera and an embedded high frequency (HF) emitter provided online images of the flying-over area on a TV. Different flight altitudes were tested from about ten meters up to few hundred meters. The resulting resolution was found to vary from less than a centimeter per pixel up to some meters per pixel. After developing, films were digitalized using a Canon CanoScan D660U scanner. 1702 by 1136 pixels images on red, green, blue (R, G, B) channels were obtained. Theses images were then saved in BMP format to avoid compression losses. Images analyzed in this paper corresponded to weed/crop competition test fields located in INRA domain in Dijon (France).

2.2. Georectification

In the case of high resolution images, only low altitudes flights were realized. Several shots were then needed to get the whole field. Landmarks (black and white draughtboard) were placed and georeferenced in the field using D-GPS coordinates (Trimble ProXRS) to locate images and also to give black and white references. A specific algorithm gave the transformation matrix between image coordinates and GPS coordinates.

3. IMAGE PROCESSING

3.1. Soil and plants discrimination

Two methods are generally employed, upon color images, to solve this problem: texture analysis or color discrimination. In most cases the first method is very efficient but the accuracy depends on soil roughness (due to clods, tires, and implements prints) and needs high cost time algorithms. The second method is based on the color properties between soil and vegetation. In our case, the R, G, B color base did not appear to give accurate colorimetric information when images are acquired under natural light. Indeed, color levels depend on lightness, that has to be separated from chromatic values. The HSV (hue, saturation, value) color base allows this separation but RGB-HSV transformation appears to be nonlinear and unstable for low RGB values. Steward and Tian [9] described another color base which is a linear combination of RGB values (1). This color base was specifically developed for vegetation images,

$$\begin{bmatrix} V_1 \\ V_2 \\ I \end{bmatrix} = \begin{bmatrix} -\frac{1}{\sqrt{2}} & \frac{1}{\sqrt{2}} & 0 \\ -\frac{1}{\sqrt{6}} & -\frac{1}{\sqrt{6}} & \frac{2}{\sqrt{6}} \\ \frac{1}{\sqrt{3}} & \frac{1}{\sqrt{3}} & \frac{1}{\sqrt{3}} \end{bmatrix} \cdot \begin{bmatrix} \mathrm{R} \\ \mathrm{G} \\ \mathrm{B} \end{bmatrix}. \tag{1}$$

Equation (1) describes the base rotation. The three vectors (V_1, V_2, I) are unitary and perpendicular, so information are fully independent; I corresponds to the luminosity vector including shadows and other lightness defaults such as reflects; (V_1, V_2) provide a colorimetric plane; V_1 is defined as the difference between red and green channels. Then V_1 is positive for vegetation pixels and negative for soil pixels. In this paper only positive values of V_1 were considered.

3.2. Seed frequency characterization

Previous image treatments led to vegetation images including crops and weeds. With the assumption that crops corresponded to repetitive structures, the Fourier transform operation was tested. The Fourier transform (FT) result corresponded to the period and the rotation angle of periodic structures. For further investigation, the seed frequency have to be characterized. A sweeping line is used to find the angle of the seed frequency with the horizontal axis. Let φ be this angle, the equation of a segment starting at the origin can be written as

$$x = t\cos\varphi, \qquad y = t\sin\varphi. \tag{2}$$

The sum of the FT along this line is the integral of the FT for this angle,

$$S(\varphi) = \sum_{t}^{x\le X, y\le Y} \mathrm{FT}(x, y), \tag{3}$$

φ values were calculated from 0 to π; S is normalized by the length of the line. Figure 1a shows the values of S as a function of the frequency angle. The maximum value of S gives the angle of the frequency.

Then, the seed frequency is found using the FT for this angle. Figure 1b shows the FT for the maximum angle.

3.3. Low frequencies enhancement

First results showed that the seed-lines had often a very low frequency. As the size of the filter kernel depends on the frequency, low frequency structures involve a big kernel with inaccurate results and very long computation time. To minimize this constraint, a dilation of the lowest frequencies must be achieved. A wavelet transform allows a low frequencies enhancement without data loss. This step is

[1] Aperture of 1 : 2.8 and focal of 35 mm, 24 × 36 mm films.

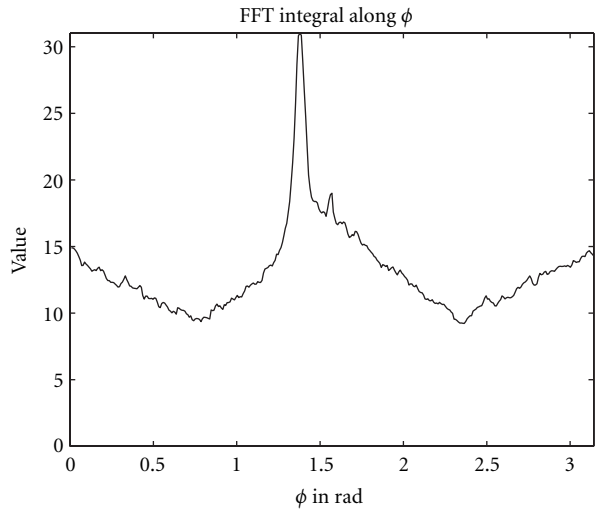

(a) Values of $S(\varphi)$ from 0 to π.

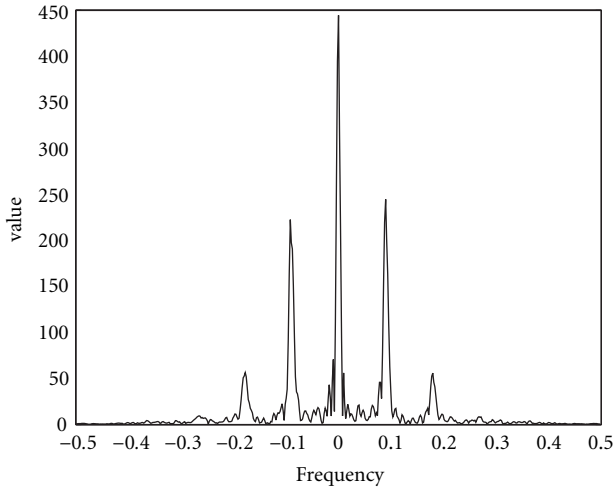

(b) FT for $\varphi = 1.3875$.

Figure 1: Seed frequency characterization.

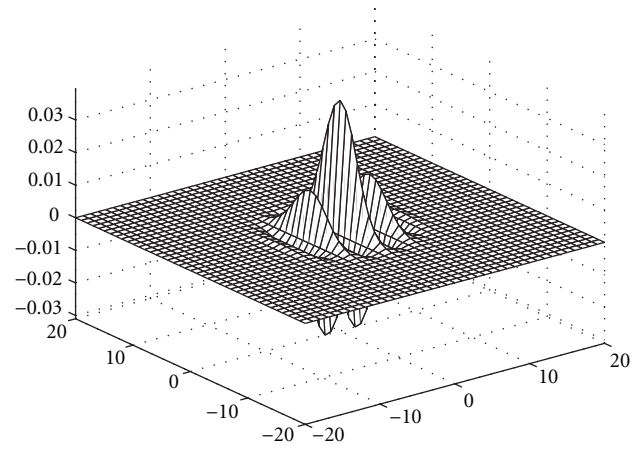

(a) Spatial representation of Gabor filter.

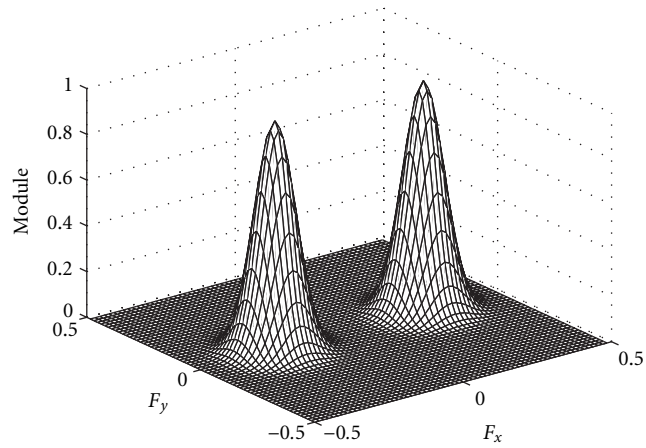

(b) Fourier transform of Gabor filter.

Figure 2: Spatial and spectral representation of Gabor filter.

recursively repeated in order to obtain a frequency compatible with an accurate filtering. In our case, a value of 1/10 is needed which corresponds to about 10 pixels between two rows.

3.4. Gabor filter

The filter is a directive band-pass filter along the axis [10]. It was centered on ω, σ_x, and σ_y set the band width, respectively, along the R_1 axis and the R_2 axis. Periodic structures with a frequency near ω and a rotation angle close to φ value were unchanged but other structures were deeply faded,

$$g(x, y) = \frac{2}{\pi\sigma_x\sigma_y} \exp\left(-\frac{R_1^2}{\sigma_x^2} - \frac{R_2^2}{\sigma_y^2}\right) \cos\left(2\pi\omega R_1\right) \qquad (4)$$

with

$$R_1 = x\cos\varphi + y\sin\varphi, \qquad R_2 = -x\sin\varphi + y\cos\varphi. \qquad (5)$$

The spatial representation of $g(x, y)$ is shown in Figure 2a, the FT in Figure 2b. It is a directive band-pass filter centered on ω, and oriented by φ. The width is defined by σ_x and σ_y. After sampling, a mask can be defined. The size of the mask depends on σ_x and σ_y. We truncate $g(x, y)$ on the interval $[-3\varphi, 3\varphi]$, where φ is the maximum of (σ_x, σ_y). We keep a good approximation with an acceptable filter size.

3.5. Gain computing

After filtering, crops would have a high value, but a simple thresholding did not give satisfying results. For example, on vegetation images crops and weeds have spread values (V_1). After filtering a low module could correspond to a weed pixel with a high value, or a crop pixel with a low value. Then we decided to compute the gain of each pixel for an accurate

Table 1: Example of gain computation for crop and weed pixels.

	Before filtering: p_{V_1}	After filtering: p_g	Gain: G
Crop	0.5	0.45	0.9
Weed	1.5	0.45	0.3

thresholding (Table 1). The gain is defined for each vegetation pixel as

$$G(x, y) = \frac{p_g(x, y)}{p_{V_1}(x, y)}. \quad (6)$$

In this equation, $p_g(x, y)$ is the module of the point after filtering, and $p_{V_1}(x, y)$, the value of this point on the vector V_1. If the gain is near 1, the point belongs to a periodic structure defined by the Gabor filter coefficients.

3.6. Results

We first decided to test this algorithm on synthesized images to confirm the validity of the method. The test images were composed of parallel line with a high-frequency noise. After this step, we tried it on images of various crops. Results depended on species and vegetation stages. Crops with an important spreading out as rape and barley gave bad results. Indeed the space between two rows was rapidly hidden by foliage during the vegetation growth. So the discrimination was almost impossible with this method. The FFT did not give the seedling frequency, so the Gabor filter cannot be tuned. On other species, the identification gave better results, and weeds can be found at early stage.

3.6.1 Low altitude image

Figure 3a shows an image of a corn field (6 per 3 meters with a resolution of around 5 mm per pixel). Some weeds can be noticed between two rows. After the processing, crops are shown in red and weeds appear in blue (Figure 3b). The end of some crop foils are detected as weeds. This default is probably due to the foil shape elongation which corresponds to a high frequency signal.

3.6.2 High altitude image

Using some field tests of INRA, we also acquired high altitude images of weed patches. The pictures represent a ground-area of about 20 per 16 meters with a resolution close to 10 cm per pixel. The crop was corn (*Zea mays*) voluntary infested with green foxtail (*Setaria viridis*) patches at various densities. The main weed patches were well recognized, but some corn foils were still detected as weeds (Figure 5).

3.6.3 Partial conclusion

The algorithm for crop row detection was efficient from a quantitative point of view. Crops were well recognized, only some foil extremities were misclassified. Weeds were also globally well classified. But, weeds located in crop rows were still detected as crops. This result led us to complete this previous spatial analysis by a spectral approach.

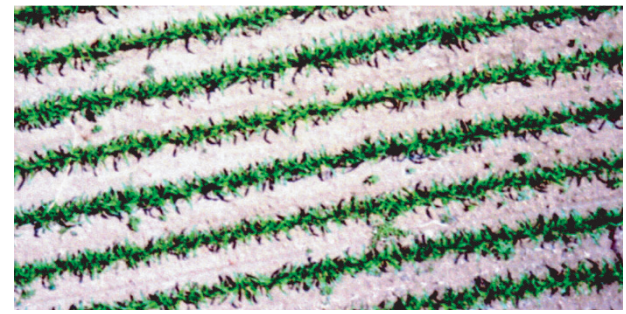

(a) Source image.

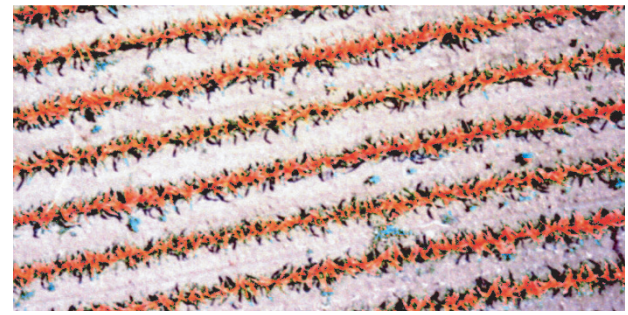

(b) Result image.

Figure 3: Low altitude image.

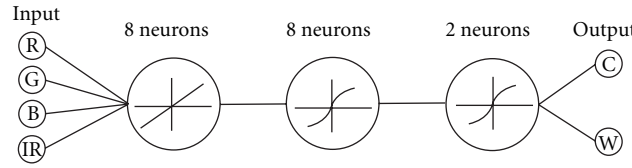

Figure 4: Neural network topology.

4. FIRST WORKS ON SPECTRAL PROPERTIES

4.1. Development of a new image acquisition device for spatial and spectral investigation

Previous works have shown possibilities of spectral information for the crop/weed discrimination [1, 11, 12]. In most studies, the visible band (red, green, blue) is completed with one or several infrared wavelengths. In the same way, we built a new acquisition device based on a CCD sensor equipped with a rotating disc holding four filters. Two filters are bandpass, one in blue (bandwidth: 50 nm, central wavelength: 500 nm) and the other in green (bandwidth: 75 nm, central wavelength: 550 nm). The two other filters are high-pass at 675 nm (red) and 750 nm (infrared) as described elsewhere [13]. The exposure time can be set at different values

Table 2: Learning rule.

	Neuron W	Neuron C
Crop	−0.9	0.9
Weed	0.9	−0.9
Soil	0	0

depending on the filter bandwidth. The four images are acquiered in less than 200 milliseconds. This device was specifically developed to be embedded in a drone where dimension and weight constraints are more important than in an aircraft [8]. First trials of this device were realized in laboratory with onion crops and various weeds.

4.2. Crops and weeds spectral separation using a neural network

The principal component analysis (PCA) was evaluated to find some difference between crops and weeds. PCA was computed only on vegetation pixels in order to obtain the greatest decorrelation between (R, G, B, IR) vectors. As a result, some slight variations on PCA vectors were found but these variations did not allow a relevant discrimination. This was probably due to a nonlinear combination of data (colors versus species). We then decided to test another classifier with nonlinear capabilities.

Considering the variability of natural images, a learning classifier can be an interesting solution [14]. In this case, few pixels are classified by the operator and the system learns the principal characteristics of this train set. For first trials, a very simple neural network was developed. The input vector is the value of the pixel on the four wavelengths. The input layer was composed of 8 cells with a linear activation function. The internal layer had the same number of neurons but with a sigmoid function allowing a nonlinear classification of data (Figure 4). Then, the output layer was composed of 2 neurons for weed and crop (W and C) with also a sigmoid function. The values of −0.9 and 0.9 were preferred than, respectively, −1 and 1 for an accurate and better learning (Table 2).

Two training sets were tested. Both have ten pixels of crops and ten pixels of weeds, but one set included ten pixels of soil. Only the pixels of vegetation were classified with the network. The results were slightly better when some soil pixels were considered for learning. In this case, the edge pixels were better classified. Figure 6a shows the infrared band of the source image. Figures 6b and 6c show the results of the two neurons. A simple threshold (equal to 0.5) was applied to obtain theses images. The network is then able to distinguish the two classes even if they are close. For example, on the top right corner (Figure 6a) a field bindweed [2] leaf is covered by an onion leaf. After classification, both plants are well classified.

[2] *Convolvus arvensis L.*

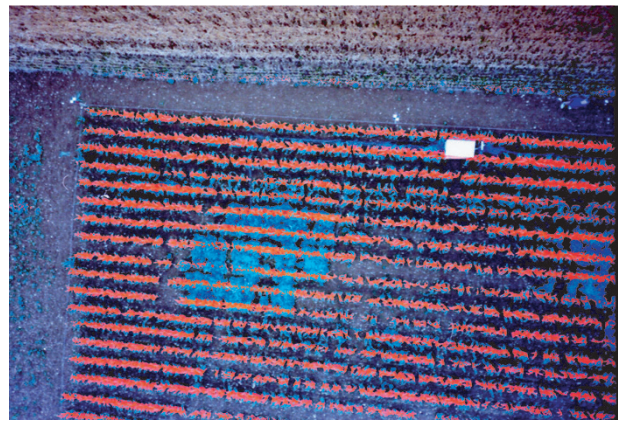

(a) Source image.

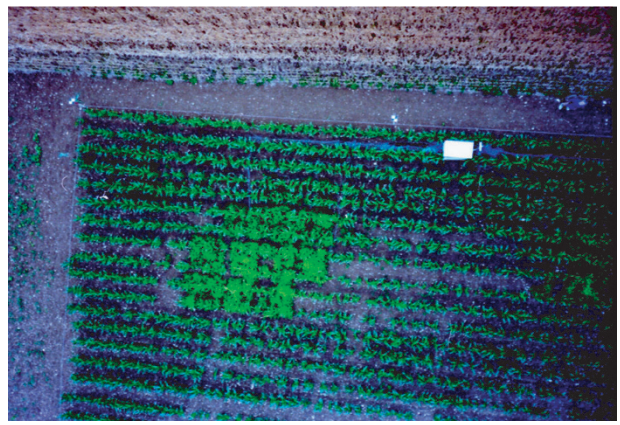

(b) Result image.

Figure 5: High altitude image.

5. CONCLUSION

A specific algorithm was developed in order to localize and discriminate weed directly from an aerial photography. The most significant result of this study consists of weed localization using spatial information given by frequency analysis. But, in most cases, weeds located in crop rows were still detected as crops.

In order to improve this previous method, species discrimination was tested through spectral information. A specific CCD camera was developed using four optical filters. With the assumption that a correlation can be suggested between spectrometric information and vegetation type (crop/weed), some classification tools were tested. Principal component analysis did not allow a good classification. Neural network gave better results due to its nonlinear activation function.

At the present time, the CCD camera is destinated to be embedded in the drone. Such an equipment will allow to acquire spectral information at a field scale and also combination with spatial information. Other kinds of information as image texture, shape analysis would be considered. The combination of all this information will be achieved using merging tools as fuzzy logic.

(a) Source image (IR channel). (b) C neuron output (Crops). (c) W neuron output (Weeds).

Figure 6: Crop/weed classification using a neural network.

ACKNOWLEDGMENTS

This project is financed with the help of ITCF (French Institute for Cereal and Forage) and the council of Burgundy. Authors also thank INRA (Dijon research center) for field disposal.

REFERENCES

[1] E. Vrindts and J. de Baerdemaeker, "Optical discrimination of crops, weeds, and soil for on-line weed detection," in *Precision Agriculture '97*, pp. 537–544, The SCI Agriculture and Environment Group, BIOS Scientific Publishers, 1997.

[2] P. Pollet, F. Feyaerts, P. Wambacq, and L. van Gool, "Weed detection based on structural information using an imaging spectrograph," in *Proc. 4th International Conference on Precision Agriculture*, pp. 1579–1591, Precision Agriculture Center, ASA-CSSA-SSSA, July 1998.

[3] D. M. Woebbecke, G. E. Meyer, K. von Bargen, and D. A. Mortensen, "Shape features for identifying young weeds using image analysis," *Transactions of the ASAE*, vol. 38, no. 1, pp. 271–281, 1995.

[4] S. Yonekawa, N. Sakai, and O. Kitani, "Identification of idealized leaf types using simple dimensionless shape factors by image analysis," *Transactions of the ASAE*, vol. 39, no. 4, pp. 1525–2533, 1996.

[5] A.-G. Manh, G. Rabatel, L. Assemat, and M.-J. Aldon, "In-field classification of weed leaves by machine vision using defomable templates," in *Proc. 3rd European Conference on Precision Agriculture*, pp. 599–604, Agro Montpellier, France, 2001.

[6] A.-G. Manh, G. Rabatel, L. Assemat, and M.-J. Aldon, "Weed leaf image segmentation by deformable templates," *J. Agric. Eng. Res.*, vol. 80, no. 2, pp. 139–146, 2001.

[7] R. H. Biller, A. Hollstein, and C. Sommer, "Precision application of herbicides by use of optoelectronics sensor," in *Proc. 1st European Conference on Precision Agriculture*, vol. 2, pp. 451–458, Technology IT and Management, Warwick University, UK, 1997.

[8] L. J. Rew, D. W. Lamb, M. M. Weedon, J. L. Lucas, R. W. Meed, and D. Lemerle, "Evaluating airborne multispectral imagery for detecting wild oats in a seedling triticale crop," in *Precision Agriculture '99*, pp. 265–274, The SCI Agriculture and Environment Group, Sheffield Academic Press, 1999.

[9] B. L. Steward and L. F. Tian, "Machine-vision weed density estimation for real-time outdoor lighting conditions," *Transactions of the ASAE*, vol. 42, no. 6, pp. 1897–1909, 1999.

[10] Y. Hamamoto, S. Uchimura, M. Watanabe, T. Yasuda, Y. Mitani, and S. Tomita, "A Gabor filter-based method for recognizing handwritten numerals," *Pattern Recognition*, vol. 31, no. 4, pp. 395–400, 1998.

[11] F. Feyarts, P. Pollet, L. van Gool, and P. Wambacq, "Sensor for weed detection based on spectral measurements," in *Proc. 4th International Conference on Precision Agriculture*, pp. 1537–1548, Precision Agriculture Center, ASA-CSSA-SSSA, 1999.

[12] R. Zwiggelaar, "A review of spectral properties of plants and their potential use for crop/weed discrimination in row-crops," *Crop Protection*, vol. 17, no. 3, pp. 189–206, 1998.

[13] P. Navar, "Conception et réalisation d'une caméra multispectrale," Memoire d'ingénieur, Conservatoire National des Arts et Métiers, Centre régional associé de Saône et Loire, France, 2001.

[14] D. Moshou, H. Ramon, and J. de Baerdemaeker, "Neural network based classification of different weeds species and crops," in *Proc. 2nd European Conference on Precision Agriculture*, pp. 275–284, The SCI Agriculture and Environment Group, Sheffield Academic Press, 1999.

Jean-Baptiste Vioix was born in Troyes, France, on September 11, 1977. He received the Master degree on image processing at University of Burgundy in 2000. He applies for a Ph.D. on image analysis. His research deals with development of a new sensor for weed detection.

Jean-Paul Douzals was born in Strasbourg, France, on February 26, 1966. He received an Engineer Diploma in agriculture engineering in 1988 and obtained his Ph.D. at the University of Burgundy in 1999. Since 2000 he is involved in researches concerning sensors and processes for precison agriculture in a joined research team with Cemagref, a French research institute for agriculture engineering, water and forest. Main research fields are sensors development (with an increasing involvement of image analysis), farm implements improvements, and localization tools (such as GPS).

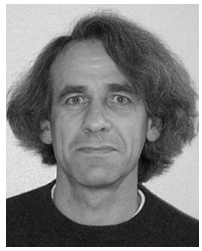

Fred Truchetet was born in Dijon, France, on October 13, 1951. He received the Master degree in physics at Dijon University, France, in 1973 and a Ph.D. in electronics at the same University in 1977. He was for two years with Thomson-CSF as a Research Engineer and he is currently full Professor in Le2i, Université de Bourgogne (France) and CNRS, where he leads the image processing group. His research interests are focused on image processing for artificial vision inspection and particularly on wavelets transform, multiresolution edge detection and image compression. He has authored and coauthored more than 150 publications, three books and holds one patent. He is member GRETSI, ASTI, IEEE, SPIE, Chairman of SPIE's conference on wavelet applications in industrial processing, and member of some technical committees of international conferences in the area of computer vision.

Louis Assémat received his Ph.D. in plant ecology from Montpellier University in 1978. After postdoctoral studies in Japan at the National Institute of Genetics in Mishima and in Great Britain at the School of Plant Biology in Bangor (North Wales), he joined the Weed Science Department at the National Institute of Agronomic Research (INRA) in Dijon. His present interests concern plant cover structure and competition between species, their link with image analysis techniques and applications to precision agriculture for weed control.

Jean-Philippe Guillemin was born in France, on April 8, 1966. He received the Master degree in biology at Franche-Comté University in 1989 and the Ph.D. in biology (organism interaction) at Burgundy University, in 1994. He was assistant professor on Agronomy in ENESAD (Etablissement National d'Enseignement Supérieur Agronomique de Dijon). His research is realized about study of competition between crop and weed and about management of weed in precision agriculture